Black Hole Winds at All Scales
Proceedings IAU Symposium No. 378, 2024
G. Bruni, M. Diaz Trigo, S. Laha & K. Fukumura, eds.
doi:10.1017/S1743921323003265

Super massive black hole and host galaxy growth at the onset of strong feedback at $z = 6 - 7.5$

Chiara Feruglio[1], Manuela Bischetti[2], Roberta Tripodi[1,2], Fabrizio Fiore[1], Enrico Piconcelli[3] and Luca Zappacosta[3]

[1]INAF - Osservatorio Astronomico di Trieste, Via G. Tiepolo 11, I-34143 Trieste, Italy
email: chiara.feruglio@inaf.it

[2]Dipartimento di Fisica, Università di Trieste, Sezione di Astronomia, Via G.B. Tiepolo 11, I-34131 Trieste, Italy

[3]INAF - Osservatorio Astronomico di Roma, Via Frascati 33, I-00040 Monte Porzio Catone, Italy

Abstract. The first quasars at the Reionisation Epoch, z∼6-7.5, probe the early stages of supermassive black holes and host galaxy assembly. In this paper, we present recent results, exploiting VLT, ALMA and NOEMA observations, that allow us to constrain the onset of strong black hole feedback, the dust properties and star formation rates in high redshift quasars with unprecedented accuracy. These results highlight the strategic importance of ALMA high frequency (i.e. Band 9 and 8) observations to obtain a reliable overview of the host galaxy and supermassive black hole growth out to the highest redshifts.

Keywords. Quasars, Supermassive black holes, AGN host galaxies, Broad-absorption line quasar, High-redshift galaxies, Galaxy evolution

1. Introduction

Luminous quasars, powered by accretion onto supermassive black holes (SMBHs), already exist at the Epoch of Reionisation (EoR), when the Universe was only 0.5-1 Gyr old (Fan *et al.* 2022). Their BH masses are as large as those of luminous quasars at lower redshift, $M_{BH} = 10^9 - 10^{10}$ $M_\odot$, meaning that BH growth had to be a fast process, and had to stop with a similarly high efficiency after the rapid build-up (Volonteri & Begelman 2010; Johnson & Haardt 2016). These huge BHs are overmassive compared to their host galaxies, with respect to the local BH mass - galaxy mass relation, suggesting that BH growth is dominating over galaxy growth in these systems.

Some feedback mechanism is then needed to slow down and suppress BH growth, leading to the symbiotic evolution observed in the local Universe. Candidate processes are inefficient gas accretion and/or feedback through BH winds (van der Vlugt & Costa 2019). At the same time, the host galaxies of high-z quasars are likely growing rapidly, which is also suggested by the recent JWST discovery of an excess of galaxies compared to the UV luminosity function predictions (Adams *et al.* 2023; Castellano *et al.* 2022; Finkelstein & Bagley 2022). The onset of significant BH feedback hampering BH growth would mark the transition from BH dominance to BH-and-galaxy symbiotic growth phases. Cosmological, hydrodynamic simulations of early BH and galaxy evolution support this scenario by identifying z∼6-7 as the transition epoch during which

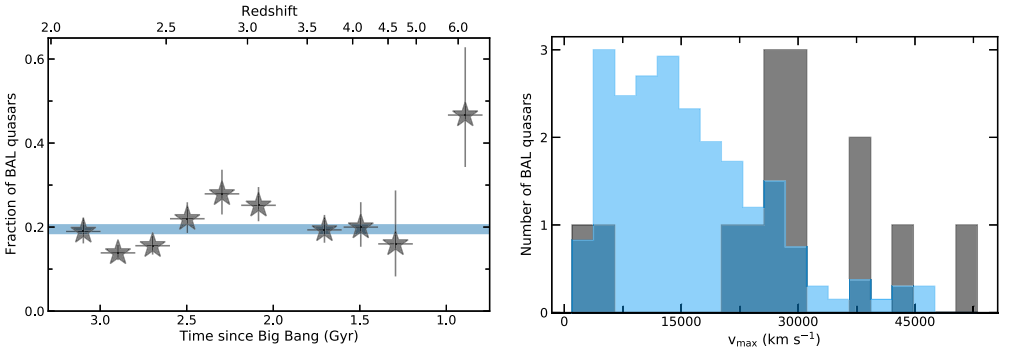

Figure 1. Left panel: Fraction of BAL quasars as a function of cosmic time, from 0.8 to 3.2 Gyr, in bins of ~ 200 Myr, based on the quasar sample in Bischetti *et al.* 2023. The shaded region corresponds to the BAL fraction measured at $2.1 < z < 4.6$ in Bischetti *et al.* 2022. Top axis indicates the corresponding redshift. Right panel: the BAL velocity distribution, parametrised here with the maximum BAL velocity, v_{max}, for the SDSS sample (blue histogram) and the XQR-30 sample (grey histogram).

quasar feedback increases in strength and starts to significantly slow down BH growth (Costa *et al.* 2018; Hu *et al.* 2022; Ishibashi & Fabian 2023).

To put this scenario into a quantitative observational framework it is necessary to accurately measure galaxy masses and growth rates and compare them to the BH growth rates, so to derive the mean evolutionary paths of quasars in the $M_{\rm BH} - M_{\rm dyn}$ plane, and verify where the BH-dominance curve changes slope, thus leading to the SMBH-host galaxy symbiotic growth. Luminous quasars at EoR may be the tip of the iceberg of a large AGN population, but allow the investigation of the BH accretion process and its feedback on the host galaxy at its extreme, and in the cleanest way (Fiore *et al.* 2017; Bischetti *et al.* 2017). The recent JWST discovery of many AGN at high redshift suggests that the AGN fraction at high z is larger than previously thought (Übler *et al.* 2023), showing that BH dominance may not only be in place for BHs with $\rm M_{BH} > 10^9$ $\rm M_\odot$, but also for less massive ones, and suggesting that luminous quasars likely represent the bright end of a population of smaller systems in which the BH grows faster than the host galaxy (Harikane *et al.* 2023; Kocevski *et al.* 2023).

In this paper we present an overview on recent results on strong quasar feedback (Sec. 2), and on the concurrent growth of SMBH and their host galaxies in quasars at $z > 6$ (Sec. 3).

We adopt a ΛCDM cosmology from the Planck Collaboration (2018): $H_0 = 67.4$ km s^{-1} Mpc^{-1}, $\Omega_m = 0.315$ and $\Omega_\Lambda = 0.685$.

2. The onset of strong quasar feedback at the Reionisation Epoch

Bischetti *et al.* (2022) analysed quasars from the X-shooter legacy survey of Quasars at Reionisation (D'Odorico *et al.* 2023), to investigate the prevalence and kinematics of BH-driven outflows as traced by Broad Absorption Line (BAL) features at $z > 6$. They analysed also 1905 luminous (bolometric luminosity $L_{\rm bol} \gtrsim 10^{46.5}$ erg s^{-1}) quasars at $z = 2.1 - 5$, drawn from the Sloan Digital Sky Survey (Shen *et al.* 2011), using the same methodology as for the the high-redshift XQR-30 sample, to derive the evolution of the BAL fraction with cosmic time. XQR-30 is a sample of 30 spectra of quasars probing the EoR ($5.8 \leq z \leq 6.6$) observed at high resolution ($R \sim 10,000$) and high signal-to-noise ratio (SNR $\sim 11 - 41$ per bin of 10 km s^{-1}) within an ESO XSHOOTER Large Programme of 248 h. The XQR-30 observations were complemented with all the available

https://doi.org/10.1017/S1743921323003265 Published online by Cambridge University Press

XSHOOTER archival observations, to form a total sample of 42 quasars that represents the state-of-the-art observational database for the studies of the second-half of the reionization process with quasar spectra.

Figure 1 shows the evolution of the BAL quasar fraction across the redshift range $2.1 < z < 6.6$ probed by the quasar sample examined in Bischetti *et al.* (2022, 2023). The BAL fraction is approximately constant at $z \lesssim 4.5$ with a median value of $\sim 20\%$, whereas is higher by a factor of about 2.5 at $z \gtrsim 6$ (Bischetti *et al.* 2022). The lack of data at $z \sim 5$ prevents us from assessing whether the decrease in the BAL fraction at $z < 6$ is smooth, consistently with secular evolution of the BH accretion properties, or whether it rapidly drops after $z \sim 6$, due to efficient BH feedback occurring at $z \sim 6$.

We also observe a redshift evolution of the BAL kinematics, as the wind velocity increases at $z \gtrsim 4$. The typical BAL velocities at $z \sim 6$ are indeed a factor of 2-3 higher than those at $z < 4$ (Figure 1, right panel). These trends are consistent with BALs being more easily accelerated at early cosmic epochs, perhaps owing to a dustier or denser galaxy medium (Bischetti *et al.* 2023). By investigating the dependence of the BAL kinematics on the quasar luminosity and accretion rate, we were able to exclude that the redshift evolution is due to different quasar prperties in the sample.

These more common and faster BAL outflows at $z \sim 6$ may witness the rise of the feedback age, owing to the injection of large amounts of energy in the host galaxy interstellar medium (ISM), in agreement with expectations from galaxy evolution models (van der Vlugt & Costa 2019; Inayoshi *et al.* 2022). We conclude that BAL winds appear fundamental tools to assess importance of BH feedback at high redshift. However, this method also suffers from an intrinsic limitation, because the broad and often saturated BAL troughs associated with CIV prevent us from obtaining an accurate measurement of the outflowing gas mass, and hence of the energy injected into the galaxy ISM (Dunn *et al.* 2012; Borguet *et al.* 2013). To derive a rough estimate of the energy involved in BAL winds, we may assume that outflow masses at $z \sim 6$ are similar to those measured using unsaturated absorption lines in $z \sim 2$ BAL quasars (Moe *et al.* 2009; Dunn *et al.* 2010). Under this assumption, we find that BAL quasars at $z \sim 6$ globally inject about 20 times more energy with respect to $z \sim 2-4$ quasars (Bischetti *et al.* 2022) in the surrounding ISM, suggesting a phase of efficient BH feedback occurring at $z \sim 6$. The energy injected by these BAL outflows will likely suppress gas accretion and slow down BH growth (Torrey *et al.* 2020). This result represents the first observational evidence of an evolution that has so far only been predicted by cosmological simulations of the early assembly of bright quasars, in which SMBHs in bright quasars grow with accretion rates close to the Eddington limit or beyond at very high redshift ($z >> 6$, (Inayoshi *et al.* 2016; Pezzulli *et al.* 2016), while around $z = 6$ BH growth significantly slows down owing to the rise of strong feedback.

Evidences of strong feedback in these high redshift quasars come also from observations of the cold gas component, for which it is easier to derive the mass and energy rate properties. Figure 2 shows the [CII] 158 μm emission line from the cold ISM of quasar SDSS J2310+1855 (Tripodi *et al.* 2022). In this quasar, the high-velocity blue- and redshifted emission that is seen in the emission line profile are spatially located in the nuclear region, and do not follow the rotation curve of the main disk. The high excess in LOS velocity between these components and the best-fit disk ($v_{\rm LOS,disk} \sim 100$ km s^{-1}) suggests that these blue- and red wings are due to a cold gaseous outflow, for which we estimate a outflow rate in the range $\dot{M}_{\rm out} \approx 1800-4500$ M$_\odot$ yr^{-1}, a kinetic power of $\dot{E}_{\rm out} = \frac{1}{2}\dot{M}_{\rm out} \times v_{\rm out}^2 = (1.5-3.7) \times 10^{44}$erg s^{-1}, and a wind momentum load $\frac{\dot{P}_{\rm out}}{\dot{P}_{\rm AGN}} = \frac{\dot{M}_{\rm out} \times v_{\rm out}}{L_{\rm bol}/c} = 0.6-1.4$, where we adopted a bolometric luminosity of

https://doi.org/10.1017/S1743921323003265 Published online by Cambridge University Press

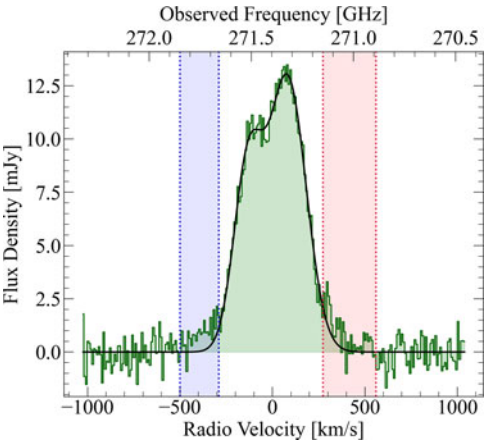

Figure 2. The [CII] 158 μm emission line profile of quasar SDSS J2310+1855 at $z = 6.0$ shows excess emission with respect to the gaussian best fit at the red and blue sides of the line. This excess emission is interpreted as evidence of a fast galactic outflow of dense molecular material (Tripodi *et al.* 2022).

$L_{\rm bol} = 3.13 \times 10^{47}$erg s^{-1}, derived from the rest-frame continuum at 3000 Å Bischetti *et al.* (2022) and the bolometric correction from Runnoe *et al.* (2012).

It is worth noting that this quasar hosts a ionised wind traced by a C IV BAL system with velocity $v_{\rm BAL} = 26900$ km s^{-1} (Bischetti *et al.* 2022), whose energy cannot be quantified due to the arguments discussed above, and a dense molecular outflow seen in absorption through blue-shifted (P-Cygni) profile in both OH 199μm and OH$^{+}(1_1 - 0_1)$ molecular transitions, probing cold and dense molecular material (Butler *et al.* 2023; Shao *et al.* 2022). These results suggest that outflows in these high redshift luminous quasars are truly multiphase. Further observations of molecular and ionic transitions with ALMA and NOEMA have the potential to assess whether there is a one-to-one correspondence between ionised winds traced by BAL systems and galaxy-scale outflows probed by molecular an ionic species in the far-infrared.

3. The host galaxy growth in $z > 6$ quasars

The host galaxy growth rate may be approximated by the ratio of the star formation rate to the total mass of the system, SFR/M$_{\rm host}$, where $M_{\rm host} = M_{\rm gas} + M_{*}$. We use $M_{\rm g+s}$, instead of $M_{\rm dyn}$, since the BH mass may not be negligible in some quasars hosting very massive BH. For example, quasar SDSS J0100+2802 has a very heavy BH, with $M_{\rm BH} \sim 40\% M_{\rm dyn}$ (Wang *et al.* 2019). Directly measuring the stellar mass M_{*} from observations has been out of reach so far for high redshift quasars, and can only be approximately evaluated by subtraction $M_{\rm dyn} - M_{\rm BH} - M_{\rm gas}$. A primary probe of molecular reservoirs, which dominate the $M_{\rm gas}$ term, are the carbon monoxide (CO) rotational transitions. At $z \sim 6 - 7.5$ the CO J=6-5 and 7-6 are conveniently redshifted at ~ 3 mm, and therefore are easily observable using ALMA and NOEMA. A recent, record-breaking CO detection was provided in the quasar J100758.264+211529.207 (Pōniuā'ena) at $z = 7.5149$ by Feruglio *et al.* (2023). Figure 3 shows the CO(6-5) and (7-6) emission line spectra from the host galaxy of the quasar obtained with NOEMA. The line luminosities correspond to a molecular mass M(H$_2$) $= \alpha_{\rm CO} \times$ L$'$CO$(6-5)$/r61 $= (2.2 \pm 0.2) \times 10^{10}$ M$_\odot$, once a conversion factor $\alpha_{\rm CO} = 0.8$ M$_\odot$ (K km s^{-1} pc^2)$^{-1}$ and a a line luminosity ratio r61 $=$ L$'$CO$(6-5)$/L$'$CO$(1-0) = 0.75$ are adopted (Carilli *et al.* 2013). These results show that CO line detection are today feasible up to the highest redshifts. When CO

https://doi.org/10.1017/S1743921323003265 Published online by Cambridge University Press

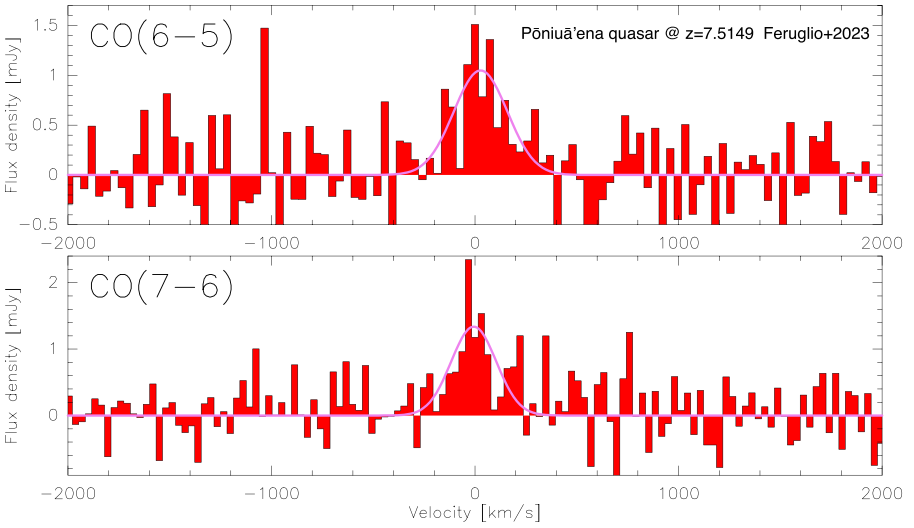

Figure 3. The CO(6-5) (upper panel) and (7-6) (lower panel) emission line spectra of the $z = 7.5149$ quasar Pōniuā'ena obtained with NOEMA Feruglio *et al.* 2023. The velocity zero point is set to the frequency 81.207 GHz for CO(6-5) and 94.734 GHz for CO(7-6). Magenta lines show the fit with a single Gaussian component.

lines are not available, one can approximate $M_{\rm host}$ with $M_{\rm dyn}$, which is routinely derived from $\sim$ kpc resolution observations using the bright [C II] line.

The SFR has proven, until recently, to be more difficult to measure. SFR in high-z quasars is typically derived by modelling the thermal dust emission probed by the (sub)-mm continuum. However, most of the values of SFR derived so far are poorly constrained because the emission peak of cold dust, located at $\lambda < 70\mu$m in the rest frame ($\nu > 4500$ GHz, i.e. > 600 GHz at $z \sim 6$) is not included in the fit (Wang *et al.* 2019; Novak *et al.* 2019), Fig. 4). This is why observations at > 600 GHz are essential to achieve tightly constrained SFR at this redshift. The commonly-used methodology is based on the modelling of the thermal dust emission with the following greybody distribution with a single temperature $T_{\rm dust}$:

$$S^{\rm obs}_{\nu/(1+z)} = \frac{\Omega}{(1+z)^3}[B_\nu(T_{\rm dust}(z)) - B_\nu(T_{\rm CMB}(z))](1 - e^{\tau_\nu}) \quad (1)$$

where $T_{\rm dust}(z) = (T^{(4+\beta)}_{\rm dust} + T^{(4+\beta)}_0[(1+z)^{(4+\beta)} - 1])^{\frac{1}{4+\beta}}$, $\tau_\nu = M_{\rm dust}k_\nu/A_{\rm gal}$ is the dust optical depth, $k_\nu = 0.45 \times (\nu/250{\rm GHz})^\beta\ cm^2\ g^{-1}$ is the dust opacity coefficient, and $A_{\rm gal}$ the galaxy area. Free parameters are the dust temperature $T_{\rm dust}$, the dust mass $M_{\rm dust}$ and the dust emissivity parameter β. Using the data typically available so far in the sub-mm range, $T_{\rm dust}$ remains unconstrained for most quasars resulting into SFR uncertain by at least a factor of ~ 5 (Wang *et al.* 2019). When only 1 or 2 data points at < 300 GHz are available, $M_{\rm dust}$ and SFR are uncertain by one order of magnitude. Similarly, assuming a fixed β leads to an estimate of $\rm M_{dust}$ with up to an order of magnitude uncertainty, and large systematic errors on important derived quantities, such as the gas-to-dust ratio and the molecular mass - thus biasing our understanding of the growth of these massive galaxies. Exceptions are the very few quasars detected by Herschel, which observed the peak of the cold dust SED emission, despite having coarse angular resolution.

ALMA Band 9 observations, in synergy with measurements at lower frequencies, represent the only method to measure reliably $\rm T_{dust}$ and SFR (Tripodi *et al.* 2023). Fig. 4 shows the first accurate $\rm T_{dust}$ determination in a $z > 6$ quasar, $\rm T_{dust} = 40 \pm 2$ K.

https://doi.org/10.1017/S1743921323003265 Published online by Cambridge University Press

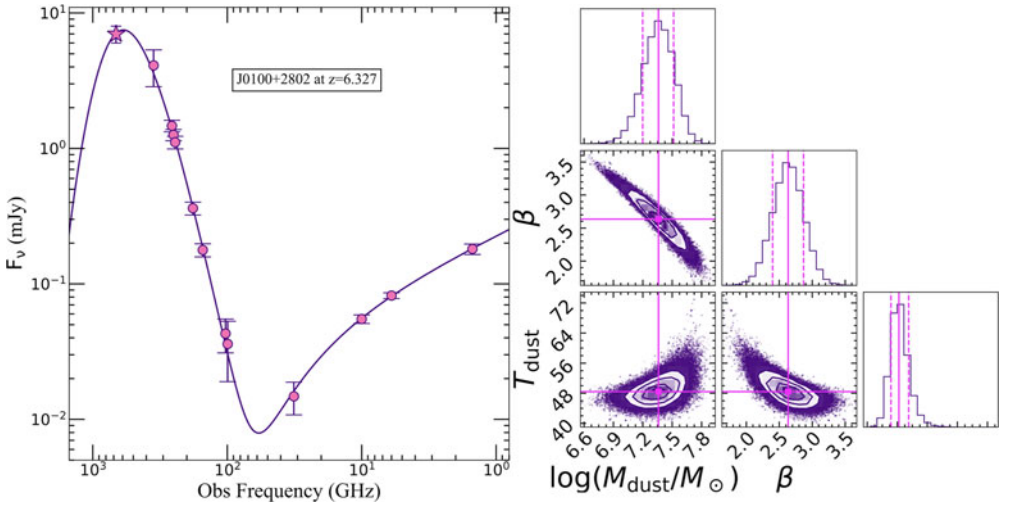

Figure 4. Left panel: Spectral Energy Distribution of quasar J0100+2802 using ALMA 670.91 GHz data (filled star, Tripodi *et al.* (2023)), the continuum fluxes from 32 GHz to 353 GHz (Wang *et al.* 2019), and at 1.5, 6 and 10 GHz (Li *et al.* 2022) (filled circles). The best-fitting curve is shown by the solid line. Right panel: posterior probability distributions of $T_{\rm dust}$, $M_{\rm dust}$, β. Solid lines indicate the best-fitting value for each parameter. Dashed lines mark the 16th and 84th percentiles for each parameter.

We estimate the total infrared (TIR) luminosity for the best-fit model by integrating from 8 to 1000 μm rest-frame, obtaining $L_{\rm TIR} = 5.30 \pm 0.64 \times 10^{12}$ L$_\odot$. Observations and radiative transfer simulations suggest that the radiative output of luminous QSOs substantially contributes to dust heating on kpc scale (Schneider *et al.* 2015; Di Mascia *et al.* 2021; Walter *et al.* 2022). Duras *et al.* (2017) showed that on average $\sim 50\%$ of the total IR luminosity in QSOs with $L_{\rm bol} > 10^{47}$ erg s^{-1} is due to dust heated by the AGN radiation. Applying this prescription, we obtain SFR $= 265 \pm 32$ M$_\odot$yr^{-1} for the quasar J0100+2802. These observations allowed us to derive SFR with 25% accuracy. This would not have been possible without a Band 9 observation with ALMA.

A further, important complication to be considered is represented by steep temperature gradients due to the AGN contribution to the dust heating, that are predicted by simulations (Di Mascia *et al.* 2023) and have been detected in quasars at $z = 4.4$ (Tsukui *et al.* 2023) and $z = 6.9$ (Walter *et al.* 2022). The latter suggests a higher T$_{\rm dust}$ in the center (> 130 K) while the overall SED is dominated by a colder component (T$_{\rm dust}$ $\sim$50 K). These gradients advocate for spatially resolved T$_{\rm dust}$ maps to account for AGN heating, which are also feasible today with ALMA at least for the brightest quasars at $z > 6$.

Together these ingredients allow us to evaluate the evolutionary state of the SMBH - host galaxy system. Figure 5 shows $M_{\rm BH}$ versus $M_{\rm dyn}$ for J0100+2802, J2310+1855 (Tripodi *et al.* 2022) and a compilation of QSOs at different redshifts. The majority of QSOs, including J0100+2802, lie above the local relation in the BH dominance regime (Volonteri 2012). We note that this tension can be partially softened if accounting for the uncertainties on the dynamical mass estimate, that mainly depend on the determination of the disk inclination and can be significantly high for some QSOs (Valiante *et al.* 2014; Pensabene *et al.* 2020). For quasar J0100+2802, $M_{\rm dyn}$ can be as high as 10^{12} M$_\odot$ if we account for this uncertainty. For J0100+2802, Tripodi *et al.* (2023) find $(1-\epsilon)\dot{M}_{\rm BH}/M_{\rm BH} > {\rm SFR}/M_{\rm g+s}$, suggesting that the BH is dominating the BH-galaxy growth. We note that their results do not consider the gas inflow, which is currently challenging to determine from observations. However, this term is expected to

https://doi.org/10.1017/S1743921323003265 Published online by Cambridge University Press

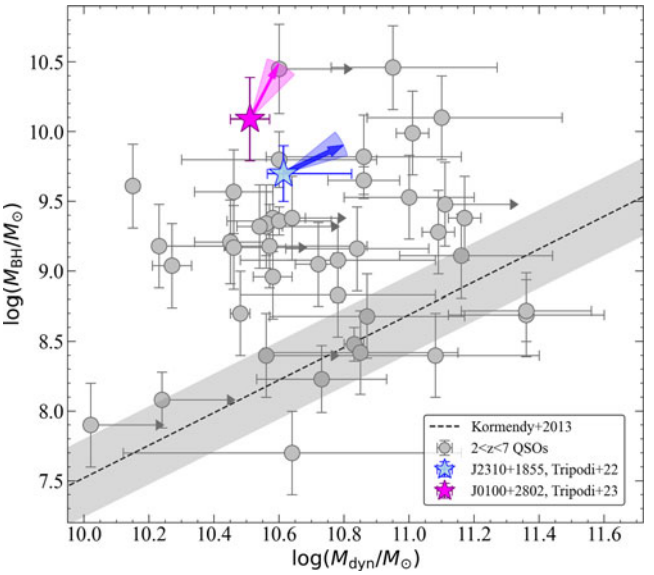

Figure 5. BH mass vs dynamical mass for J0100+28 (magenta symbol), compared with QSO J2310+18 at $z = 6.0028$ (blue symbol), and a compilation of $z \sim 2 - 7$ quasars from Tripodi *et al.* (2023) and references therein (grey symbols). The black dashed line (and shaded area) is the local relation from Kormendy & Ho (2013). For J0100+28 (J2310+18), the slope of the arrow, with its uncertainty, indicates the growth efficiency of the SMBH with respect to the growth of the host galaxy.

contribute to both SFR and $M_{\rm g+s}$, leaving their ratio mostly unaffected. Conversely, in the quasar J2310+1855 at $z \sim 6$ AGN feedback might be slowing down the accretion onto the SMBH, while the host galaxy grows fast (Tripodi *et al.* 2022; Bischetti *et al.* 2022). The different evolutionary state of J0100+2802 and J2310+1855, which are separated by only ~ 60 Myr (i.e. $\Delta z \sim 0.3$), arise mainly from the difference in their BH mass ($M_{\rm BH,J0100+28} \sim 2 \times \ M_{\rm BH,J2310+18}$) and SFR ($\rm SFR_{J0100+28} \sim 0.2 \times SFR_{J2310+18}$). As already mentioned, $\rm SFR/M_*$ is a better probe of the galaxy growth, however this is not available for most high redshift QSOs. For J0100+2802, using $\rm SFR/M_*$ would not affect our results since $M_{\rm g+s} \approx M_*$. For J2310+1855, $M_* \ll M_{\rm g+s}$, therefore it would imply an even flatter slope.

The cases of these two quasars represent two snapshots of different evolutionary phases, and are useful to illustrate the methodology that could be used to set this evolutionary scenario in a quantitative observational framework. This goal can be achieved by using a large sample of quasars at $z > 6$ and accurately measure their BH masses, dynamical masses and SFR, so to derive the mean evolutionary paths of quasars in the $M_{\rm BH} - M_{\rm dyn}$ plane.

References

Adams, N. J., Conselice, C. J., Austin, D., et al. 2023, *arXiv*, doi:10.48550/arXiv.2304.13721
Bischetti, M., Piconcelli, E., Vietri, G., et al. 2017, *A&A*, 598, A122.
Bischetti, M. and Feruglio, C. and D'Odorico, V. et al. 2022, *Nature*, 605, 7909
Bischetti, M., Fiore, F., Feruglio, C., et al. 2023, *arXiv*, doi:10.48550/arXiv.2301.09731
Borguet, B. C. J., Arav, N., Edmonds, D., et al. 2013, *ApJ*, 762, 49
Butler, K. M., van der Werf, P. P., Topkaras, T., et al. 2023, *ApJ*, 944, 134
Castellano, M., Fontana, A., Treu, T., et al. 2022, *ApJL*, 938, L15
Costa, T., Rosdahl, J., Sijacki, D., et al. 2018, *MNRAS*, 479, 2079

https://doi.org/10.1017/S1743921323003265 Published online by Cambridge University Press

Di Mascia, F., Gallerani, S., Behrens, C., et al. 2021, *MNRAS*, 503, 2349
Di Mascia, F., Carniani, S., Gallerani, S., et al. 2023, *MNRAS*, 518, 3667
D'Odorico, V., Bañados, E., Becker, G. D., et al. 2023, *MNRAS*, 523, 1399
Draine, B.T. 2003, *ARAA*, 41, 241
Dunn, J. P., Bautista, M., Arav, N., et al. 2010, *ApJ*, 709, 611
Dunn, J. P., Arav, N., Aoki, K., et al. 2012, *ApJ*, 750, 143
Duras, F., Bongiorno, A., Piconcelli, E., et al. 2017, *A&A*, 604, A67
Fan, X., Banados, E., & Simcoe, R. A. 2022, *arXiv*, doi:10.48550/arXiv.2212.06907
Finkelstein, S. L. & Bagley, M. B. 2022, *ApJ*, 938, 25
Fiore, F., Feruglio, C., Shankar, F., et al. 2017, *A&A*, 601, A143.
Harikane, Y., Zhang, Y., Nakajima, K., et al. 2023, *arXiv*, doi:10.48550/arXiv.2303.11946
Hu, H., Inayoshi, K., Haiman, Z., et al. 2022, *ApJ*, 934, 132
Inayoshi, K., Haiman, Z., & Ostriker, J. P. 2016, *MNRAS*, 459, 3738
Inayoshi, K., Nakatani, R., Toyouchi, D., et al. 2022, *ApJ*, 927, 237
Ishibashi, W. & Fabian, A. C. 2023, *MNRAS*, 519, 1931
Johnson, J. L. & Haardt, F. 2016, *PASA*, 33, e007
Kocevski, D. D., Onoue, M., Inayoshi, K., et al. 2023, *arXiv*, doi:10.48550/arXiv.2302.00012
Kormendy, J. & Ho, L. C. 2013, *ARAA*, 51, 511
Moe, M., Arav, N., Bautista, M. A., et al. 2009, *ApJ*, 706, 525
Novak, M., Bañados, E., Decarli, R., et al. 2019, *ApJ*, 881, 63
Pensabene, A., Carniani, S., Perna, M., et al. 2020, *A&A*, 637, A84
Pezzulli, E., Valiante, R., & Schneider, R. 2016, *MNRAS*, 458, 3047
Planck Collaboration et al. 2018, *arXiv*, 1807.06209
Runnoe, J. C., Brotherton, M. S., & Shang, Z. 2012, *MNRAS*, 422, 478
Schneider, R., Bianchi, S., Valiante, R., et al. 2015, *A&A*, 579, A60
Shao, Y., Wang, R., Weiss, A., et al. 2022, *A&A*, 668, A121
Shen, Y., Richards, G. T., Strauss, M. A., et al. 2011, *ApJS*, 194, 45
Torrey, P., Hopkins, P. F., Faucher-Giguère, C.-A., et al. 2020, *MNRAS*, 497, 5292
Tripodi, R., Feruglio, C., Fiore, F., et al. 2022, *A&A*, 665, A107
Tripodi, R., Feruglio, C., Kemper, F., et al. 2023, *ApJL*, 946, L45
Tsukui, T., Wisnioski, E., Krumholz, M. R., et al. 2023, *arXiv*, doi:10.48550/arXiv.2302.07272
Übler, H., Maiolino, R., Curtis-Lake, E., et al. 2023, *arXiv*, doi:10.48550/arXiv.2302.06647
Valiante, R., Schneider, R., Salvadori, S., et al. 2014, *MNRAS*, 444, 2442
van der Vlugt, D. & Costa, T. 2019, *MNRAS*, 490, 4918
Volonteri, M. & Begelman, M. C. 2010, *MNRAS*, 409, 1022
Volonteri, M. 2012, *Science*, 337, 544.
Walter, F., Neeleman, M., Decarli, R., et al. 2022, *ApJ*, 927, 21
Wang, F., Wang, R., Fan, X., et al. 2019, *ApJ*, 880, 2